Performance Analysis of Differential-Phase-Shift-Keying Optical Receivers in the Presence of In-Band Crosstalk Noise

Thomas Kamalakis and Thomas Sphicopoulos, *Member, IEEE*

***Abstract*—In-band crosstalk can pose important limitations in an all-optical wavelength-division-multiplexed (WDM) network. Recent studies have demonstrated that differential phase shift keying (DPSK), can tolerate higher in-band crosstalk-noise levels compared to amplitude shift keying (ASK). In this paper, the performance of a DPSK receiver, limited by in-band crosstalk noise, is studied theoretically. The model takes into account both the in-band crosstalk noise as well as the amplified-spontaneous-emission (ASE) noise of the optical amplifiers. The model is based on the evaluation of the moment-generating function (MGF) of the decision variable through which, the error probability (EP) can be calculated by applying the saddle point approximation. This provides a rigorous model for the evaluation of the EP of a DPSK receiver in the presence of ASE and in-band crosstalk noises. In the absence of the ASE noise, a closed-form formula for the EP is also given that is useful for estimating the error floor set by the in-band crosstalk noise.**

***Index Terms*—Crosstalk, error analysis, optical receivers, wavelength division multiplexing (WDM).**

I. Introduction

THE PERFORMANCE of wavelength-division-multiplexing (WDM) networks can be degraded by the presence of in-band crosstalk noise [1]. This noise arises at optical crossconnects because, due to their imperfect filtering characteristics, a small delayed version of the signal or a small portion of light from other channels at the same frequency (in a network with wavelength reuse) is routed along the same path as the signal. Since in-band crosstalk noise is at the same wavelength as the signal, it cannot be removed using additional filtering and can degrade the error probability (EP) at the receiver. The power of the noise is proportional to that of the signal, and hence, an increase of the signal power does not change the signal-to-crosstalk ratio (defined as the ratio of the power of the signal to the power of the crosstalk). This sets a lower limit in the value of the EP [2], usually referred to as an error floor, which can limit the number of nodes of a WDM network.

Due to its importance, in-band crosstalk noise has been extensively studied in the literature (see [3]–[10] and references therein) in the case of amplitude-shift-keying (ASK) signal modulation. At the receiving photodiode, two in-band noise contributions must be taken into account [7]: one resulting from the beating of the signal with the optical crosstalk noise and one from the beating of the crosstalk noise with itself. The impact of in-band crosstalk was investigated using the Gaussian approximation [3] in the case of an arrayed-waveguide-grating (AWG) interconnection. The Gaussian approximation is based on the Central Limit Theorem (CLT) and assumes a large number M of interfering crosstalk components. Although the Gaussian approximation is relatively straightforward, it neglects the crosstalk–crosstalk beating noise at the receiving photodiode. An accurate noise description should consider both in-band crosstalk-noise contributions, which are statistically correlated since they originate from the same optical noise. Besides, as shown experimentally by Jiang and Roudas [9], in the presence of in-band crosstalk noise, the probability density function (pdf) of the decision variable at the receiver is asymmetric, and hence, the Gaussian model may not provide an accurate description for the noise statistics. It was recently shown that, due to the presence of the crosstalk–crosstalk beating, the decision variable asymptotically becomes a Chi-square random variable as $M \to \infty$ [10]. Hence, the in-band crosstalk noise cannot be assumed Gaussian, even in this limit.

Recently, it was experimentally demonstrated that differential phase shift keying (DPSK) [11] can increase the system tolerance to in-band crosstalk compared to ASK. The above study considered a single interfering component. There are however, many practical situations, such as the passive AWG interconnection, where the number of crosstalk components can be quite large. Therefore, the performance of the DPSK receiver in the presence of many crosstalk components must be considered. It should also be noted that the DPSK modulation format increases the system tolerance to fiber-induced nonlinear distortion [12]. Therefore, the DPSK format deserves a more detailed analysis, since it constitutes an attractive candidate for future WDM-network implementation.

In this paper, the performance of a DPSK receiver, limited by in-band crosstalk and amplified-spontaneous-emission (ASE) noises, is theoretically analyzed assuming a large number of in-band interfering components. A closed-form formula for the moment-generating function (MGF) of the decision variable is derived. This formula can be used to estimate the EP using the saddle point approximation [13]. In addition, in the case where the ASE noise is neglected, a closed-form formula is given for the EP. This formula can be used to estimate the error floor set by the in-band crosstalk noise in a DPSK receiver.

Manuscript received January 18, 2005; revised June 21, 2005.

The authors are with the Department of Informatics and Telecommunications, University of Athens, Athens GR-15784, Greece (e-mail: thkam@di.uoa.gr).

Digital Object Identifier 10.1109/JLT.2005.859429

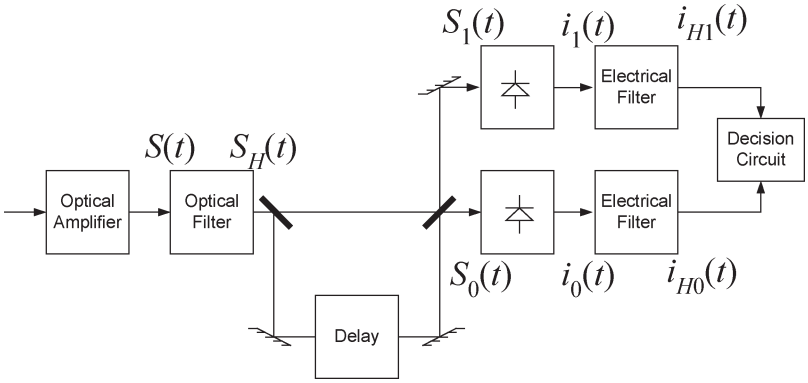

Fig. 1. Typical DPSK receiver diagram.

II. Receiver Model

In this section, the DPSK receiver model in the presence of in-band crosstalk noise will be presented. This model will be used in the next sections to evaluate the decision variable and its MGF. A typical DPSK receiver [13] is depicted in Fig. 1. At the output of the optical amplifier, the optical field $S(t)$ is given by

$$S(t) = S_0(t) + S_X(t) + N_{\text{ase}}(t) \tag{1}$$

where $S_0(t)$ is the desired DPSK signal. Assuming two consecutive bit intervals, $S_0(t)$ is written as

$$S_0(t) = c_0 \left(\mathrm{e}^{j\theta_{0a}} g(t) + \mathrm{e}^{j\theta_{0b}} g(t+T)\right) \mathrm{e}^{j\varphi_0} \tag{2}$$

for values of t inside the interval $[-T, T]$, where T equals a single bit duration. In (2), the random phase ϕ_0 is due to the laser phase noise and is assumed uniform in $[0, 2\pi]$, $g(t)$ is an arbitrary pulse shape that is considered zero outside the interval $[0, T]$. If the bit B_a to be transmitted in $[0, T]$ is the same with the bit B_b of the previous interval $[-T, 0]$, then $\theta_{0a} - \theta_{0b} = 0$, while if $B_b \neq B_a$, then $\theta_{0a} - \theta_{0b} = \pi$, i.e., the information is coded as phase shifts between the successive bit intervals. The constant c_0 is the amplitude of the signal. The field $S_X(t)$ is the in-band crosstalk noise, and is written as

$$S_X(t) = \sum_{m=1}^{M} c_m \left(\mathrm{e}^{j\theta_{ma}} g(t) + \mathrm{e}^{j\theta_{mb}} g(t+T)\right) \mathrm{e}^{j\varphi_m} \tag{3}$$

where M is the total number of crosstalk components, the phases θ_{ma} and θ_{mb} designate the bit changes of the crosstalk component m, c_m is its amplitude, and ϕ_m is due to the phase noise. The phases ϕ_m for $1 \leq m \leq M$, are uniform random variables inside $[0, 2\pi]$, independent of each other and of ϕ_0. The field $N_{\text{ase}}(t)$ is the ASE noise of the optical amplifier and can be modeled as an additive white Gaussian stochastic noise process. The field $S(t)$ is filtered by the optical filter and the filtered optical field $S_H(t)$ is given by

$$S_H(t) = \sum_{m=0}^{M} c_m \left(\mathrm{e}^{j\theta_{ma}} g_H(t) + \mathrm{e}^{j\theta_{mb}} g_H(t+T)\right) \mathrm{e}^{j\varphi_m} + n(t) \tag{4}$$

where $g_H(t)$ and $n(t)$ are the filtered versions of $g(t)$ and $N_{\text{ase}}(t)$, respectively. The field $S_H(t)$ is directed to a Mach–Zehnder interferometer, which forms two auxiliary optical signals $S_1(t) = [S_H(t) + S_H(t-T)]/2$ and $S_0(t) = [S_H(t) - S_H(t-T)]/2$. Each signal is fed to a separate photodiode. If the quantum efficiency is taken equal to unity, and if the intensity $|S_1(t)|^2$ is measured in photons per second, then the induced photocurrent $i_1(t)$ at the upper photodiode is $i_1(t) = 1/2|S_1(t)|^2$ (photoelectrons/s), where the factor 1/2 is due to the complex notation adopted for the optical fields [13]. The photocurrent $i_1(t)$ is directed to an electrical filter. Assuming an integrate-and-dump filter, the photocurrent at the output of the filter at time $t = T$, is given by

$$i_{H1}(T) = \frac{1}{T}\int_0^T i_1(t')dt' = \frac{1}{8T}\int_0^T |S_H(t') + S_H(t'-T)|^2 \, dt. \tag{5}$$

The photocurrent $i_0(t) = 1/2|S_0(t)|^2$ at the lower photodiode passes through a similar electrical filter and the filtered photocurrent is

$$i_{H0}(T) = \frac{1}{T}\int_0^T i_0(t')dt' = \frac{1}{8T}\int_0^T |S_H(t') - S_H(t'-T)|^2 \, dt. \tag{6}$$

The filtered photocurrents $i_{H1}(t)$ and $i_{H0}(t)$ are then fed to a decision circuit. At $t = T$, the value of the decision variable $D = D(T) = i_{H1}(T) - i_{H2}(T)$ is used to infer the value of the received bit. Using (5) and (6), it is easy to show that

$$D = \frac{1}{2T}\mathrm{Re}\left\{\int_0^T S_H(t') S_H^*(t'-T)dt'\right\}. \tag{7}$$

Equations (1)–(7) describe the DPSK-receiver model and will be used to derive a closed-form expression for the MGF, $M_D(s) = \langle \mathrm{e}^{sD} \rangle$ in the presence of the ASE noise.

III. Estimation of the Decision Variable

Using (7), one can derive an expression for the decision variable that contains both the ASE and the in-band crosstalk

contribution. To accomplish this, the ASE noise is first expanded in a Fourier series. Then, four auxiliary random variables that contain the contribution of the crosstalk noise are defined, and the decision variable is expressed in terms of these random variables.

A. Expansion of the ASE Noise

To estimate the decision variable in the presence of the ASE noise, the amplifier noise after the optical filter $n_1(t) = n(t)$ inside $[0, T]$ is written as [13]

$$n_1(t) = \sum_{k=-\infty}^{+\infty} N_k \mathrm{e}^{j\frac{2\pi}{T}kt} \tag{8}$$

where $N_k = N_{kr} + jN_{ki}$ are the Fourier components of $n_1(t)$ and N_{kr} and N_{ki} are independent Gaussian random variables [13] having zero mean value and standard deviation given by

$$\left\langle N_{kr}^2 \right\rangle = \left\langle N_{ki}^2 \right\rangle = \sigma_k^2 = \frac{n_{\mathrm{sp}}(G-1)H^2\left(\frac{k}{T}\right)}{T} \tag{9}$$

where $H(k/T)$ is the transfer function of the optical filter at $f = k/T$, and H/kT is for simplicity assumed real. The ASE noise inside $[-T, 0]$, $n_2(t)$ can be written in a similar manner in terms of its Fourier components $M_k = M_{kr} + jM_{ki}$.

$$n_2(t) = \sum_{k=-\infty}^{+\infty} M_k \mathrm{e}^{j\frac{2\pi}{T}kt} \tag{10}$$

The standard deviation of M_{kr} and M_{ki} is the same as that of N_{kr} and N_{ki}. The pulse $g_H(t)$ can also be written as

$$g_H(t) = \sum_{k=-\infty}^{+\infty} g_k \mathrm{e}^{j\frac{2\pi}{T}kt} \tag{11}$$

where g_k are the Fourier coefficients of $g_H(t)$.

B. Definition of the Auxiliary Random Variables

To facilitate the analysis, four auxiliary random variables are defined

$$X_a = c_0 e_{0a}\cos\phi_0 + \sum_{m\geq 1} c_m e_{ma}\cos\phi_m \tag{12a}$$

$$X_b = c_0 e_{0b}\cos\phi_0 + \sum_{m\geq 1} c_m e_{mb}\cos\phi_m \tag{12b}$$

$$Y_a = c_0 e_{0a}\sin\phi_0 + \sum_{m\geq 1} c_m e_{ma}\sin\phi_m \tag{12c}$$

$$Y_b = c_0 e_{0b}\sin\phi_0 + \sum_{m\geq 1} c_m e_{mb}\sin\phi_m \tag{12d}$$

where $e_{ma} = \exp(j\theta_{ma})$ and $e_{mb} = \exp(-j\theta_{mb})$. The field $S_H(t)$ inside $[0, T]$ is

$$S_H(t) = \sum_k \left[(X_a + jY_a)g_k + N_k\right]\mathrm{e}^{j\frac{2\pi}{T}kt} \tag{13}$$

where $t \in [0, T]$ and to derive (13), one uses (8), (11), and (12). Similarly, the optical field $S_H(t-T)$ is written as

$$S_H(t-T) = \sum_k \left[(X_b + jY_b)g_k + M_k\right]\mathrm{e}^{j\frac{2\pi}{T}kt}. \tag{14}$$

Equation (13) reveals one fundamental difference between the ASE and the in-band crosstalk noise. The ASE noise before the optical filter, is an additive white Gaussian noise, and hence, the N_k and M_k are uncorrelated. On the contrary, the in-band crosstalk noise is not white, since its spectral components $(X_a + jY_a)g_k$ and $(X_b + jY_b)g_k$ are correlated. Hence, when both noises are present, the total noise can behave quite differently than a white Gaussian process as will be shown in Section IV, and the error formulas derived for the ASE noise cannot be directly applied by simply accounting the in-band crosstalk noise in the signal-to-noise ratio.

One important difference between the ASE noise and the crosstalk noise is that the crosstalk noise can be much more bursty (see [11]). This may cause system outages in systems using forward error correction (FEC). So, the crosstalk-induced error floor is quite important and may be related to system outage.

C. Derivation of the Decision Variable

Applying (13) and (14) and integrating, it is easy to show that

$$\frac{1}{T}\int_0^T S_H(t')S_H(t'-T)dt' = \sum_k \left\{\left[(X_a + jY_a)g_k + N_k\right]\left[(X_b - jY_b)g_k^* + M_k^*\right]\right\}. \tag{15}$$

Taking the real part of (15) and using (7), one obtains

$$D = \frac{1}{2}\sum_k \{(x_{ka} + N_{kr})(x_{kb} + M_{kr}) + (y_{ka} + N_{ki})b(y_{kb} - M_{ki})\} \tag{16}$$

where

$$x_{ka} = \mathrm{Re}\left\{(X_a + jY_a)g_k\right\} \tag{17a}$$

$$x_{kb} = \mathrm{Re}\left\{(X_b + jY_b)g_k\right\} \tag{17b}$$

$$y_{ka} = \mathrm{Im}\left\{(X_a + jY_a)g_k\right\} \tag{17c}$$

$$y_{kb} = \mathrm{Im}\left\{(X_b + jY_b)g_k\right\}. \tag{17d}$$

Defining

$$D_{kr} = \frac{1}{2}(x_{ka} + N_{kr})(x_{kb} + M_{kr}) \tag{18a}$$

$$D_{ki} = \frac{1}{2}(y_{ka} + N_{ki})(y_{kb} - M_{ki}) \tag{18b}$$

the decision variable is written as

$$D = \sum_k (D_{kr} + D_{ki}). \tag{19}$$

Equations (18) and (19) indicate the fact that the decision variable is the sum of the random variables D_{kr} and D_{ki}. Given the values of x_{ka}, x_{kb}, y_{ka}, and y_{kb}, it is deduced that D_{ki} and D_{kr} are mutually independent and each one is a product of two independent Gaussian random variables. However, x_{ka}, x_{kb}, y_{ka}, and y_{kb} are also random variables whose statistical behavior is determined by the statistics of X_a, Y_a, X_b, and Y_b.

IV. Evaluation of the MGF of the Decision Variable

Equation (19) is the starting point for the evaluation of the MGF, $M_D(s) = \langle \mathrm{e}^{sD} \rangle$, of the decision variable D. To evaluate the MGF, the expectation of e^{sD} with respect to the ASE noise components, M_k and N_k, will first be calculated. Then, the statistical properties of X_a, Y_a, X_b, and Y_b will be used to evaluate the expectation of e^{sD} with respect to these variables as well.

A. Expectation of e^{sD} With Respect to the ASE Components

The MGFs $M_{kr}(s)$ and $M_{ki}(s)$ of D_{kr} and D_{ki}, respectively, can be computed in closed form using the formula

$$I = \frac{1}{2\pi} \int_{-\infty}^{+\infty} dx \int_{-\infty}^{+\infty} dy e^{a(x^2+y^2)+\beta xy+\gamma x+\delta y+\varepsilon}$$
$$= \frac{1}{\sigma^2\sqrt{4a^2-\beta^2}} \exp\left(\frac{\beta\gamma\delta + a(\gamma^2+\delta^2)}{4a^2-\beta^2} + \varepsilon\right) \tag{20}$$

where $a < 0$. This formula is easily derived by using [19, eq. (3.323.2)]. Using (20), one can show that

$$M_{kr}(s) = \frac{1}{\sqrt{1-\frac{\sigma_k^4 s^2}{4}}} \times \exp\left(\frac{\frac{[x_{ka}^2+x_{kb}^2]\sigma_k^2 s^2}{4} + x_{ka}x_{kb}s}{2\left(1-\frac{\sigma_k^2 s^2}{4}\right)}\right) \tag{21a}$$

$$M_{ki}(s) = \frac{1}{\sqrt{1-\frac{\sigma_k^4 s^2}{4}}} \times \exp\left(\frac{\frac{[y_{ka}^2+y_{kb}^2]\sigma_k^2 s^2}{4} + y_{ka}y_{kb}s}{2\left(1-\frac{\sigma_k^2 s^2}{4}\right)}\right). \tag{21b}$$

The MGF $M_{D|C}(s)$ of D, given the realization of the crosstalk noise, i.e., the values of x_{ka}, y_{ka}, x_{kb}, and y_{kb}, is simply the product of these MGFs, i.e.,

$$M_{D|C}(s) = \prod_{k=-\infty}^{+\infty} M_{kr}(s) \prod_{k=-\infty}^{+\infty} M_{ki}(s). \tag{22}$$

Substituting (20) and (21) in (22), one obtains

$$M_{D|C}(s) = \left(\prod_{k=-\infty}^{+\infty} \frac{1}{1-\frac{\sigma_k^4 s^2}{4}}\right) \times \exp\left(\sum_{k=-\infty}^{+\infty} \frac{\frac{(x_{ka}^2+x_{kb}^2+y_{ka}^2+y_{kb}^2)\sigma_k^2 s^2}{4} + (x_{ka}x_{kb}+y_{ka}y_{kb})s}{2\left(1-\frac{\sigma_k^4 s^2}{4}\right)}\right). \tag{23}$$

Substituting (17) into (23), the following form for $M_{D|C}(s)$ is obtained:

$$M_{D|C}(s) = C(s)\exp\left(A(s)\left[X_a^2+Y_a^2+X_b^2+Y_b^2\right] + B(s)[X_aX_b+Y_aY_b]\right) \tag{24}$$

where

$$A(s) = \sum_{k=-\infty}^{+\infty} \frac{\sigma_k^2 s^2 |g_k|^2}{8\left(1-\frac{\sigma_k^4 s^2}{4}\right)} \tag{25a}$$

$$B(s) = \sum_{k=-\infty}^{+\infty} \frac{|g_k|^2 s}{2\left(1-\frac{\sigma_k^4 s^2}{4}\right)} \tag{25b}$$

$$C(s) = \prod_{k=-\infty}^{+\infty} \frac{1}{1-\frac{\sigma_k^4 s^2}{4}}. \tag{25c}$$

To complete the evaluation of the MGF, the expected value of (24) with respect to X_a, Y_a, X_b, and Y_b must be computed, and thus, the statistical properties of the auxiliary random variables X_a, Y_a, X_b, and Y_b must first be considered.

B. Statistical Behavior of the Auxiliary Random Variables

Given the value of ϕ_0, e_{0a}, and e_{0b}, the mean values of the auxiliary variables are given by

$$m_{xa} = \langle X_a \rangle = c_0 e_{0a} \cos\phi_0 \tag{26a}$$

$$m_{xb} = \langle X_b \rangle = c_0 e_{0b} \cos\phi_0 \tag{26b}$$

$$m_{ya} = \langle Y_a \rangle = c_0 e_{0a} \sin\phi_0 \tag{26c}$$

$$m_{yb} = \langle Y_b \rangle = c_0 e_{0b} \sin\phi_0. \tag{26d}$$

Equations (26a)–(26d) are easily derived, since $\langle \cos\phi_m \rangle = \langle \sin\phi_m \rangle = 0$, for $m > 0$. To evaluate the standard deviations of σ_{xa}, σ_{xb}, σ_{ya}, and σ_{yb}, of the auxiliary random variables

X_a, X_b, Y_a, and Y_b, respectively, one uses $\langle \cos^2 \phi_m \rangle = \langle \sin^2 \phi_m \rangle = 1/2$ and $\langle e_{0a}^2 \rangle = \langle e_{0b}^2 \rangle = 1$. The result is

$$\sigma_{xa}^2 = \sigma_{ya}^2 = \sigma_{xb}^2 = \sigma_{yb}^2 = \sigma^2 = \frac{1}{2} \sum_{m \geq 1} c_m^2. \tag{27}$$

As $M \to \infty$, the random variables X_a, X_b, Y_a, and Y_b asymptotically become Gaussian as a consequence of the CLT. It is interesting to also note that as $M \to \infty$, the auxiliary random variables become statistically independent of each other. To show this, the covariance $\rho_{kl} = \langle (Z_k - \langle Z_k \rangle)(Z_l - \langle Z_l \rangle) \rangle$, where $Z_1 = X_a$, $Z_2 = X_b$, $Z_3 = Y_a$, and $Z_4 = Y_b$ can be used. If the covariance ρ_{kl} is zero for $k \neq l$, then (due to the Gaussian statistics of the variables) the variables are independent [18]. The evaluation of ρ_{kl} is relatively straightforward. For example, for $k = 1$ and $l = 2$, one has

$$\begin{aligned} \rho_{12} &= \langle (X_a - m_{xa})(X_b - m_{xb}) \rangle \\ &= \sum_{m=1}^{M} \sum_{n=1}^{M} c_m c_n \langle \cos \phi_m \cos \phi_n \rangle \langle e_{ma} e_{nb} \rangle. \end{aligned} \tag{28}$$

The variables ϕ_m are independent, and since $\langle \cos \phi_m \rangle = 0$, $\langle \cos^2 \phi_m \rangle = 1/2$, one obtains $\langle \cos \phi_m \cos \phi_n \rangle = 1/2 \delta_{mn}$, where δ_{mn} is Kronecker's delta ($\delta_{mn} = 0$ for $m \neq n$ and $\delta_{mm} = 1$). Using the fact that $\langle e_{ma} e_{mb} \rangle = \langle \exp(j(\theta_{ma} - \theta_{mb}) \rangle = 1/2(+1) + 1/2(-1) = 0$, it is easy to ascertain that $\rho_{12} = 0$. In a similar manner, it is possible to show that $\rho_{kl} = 0$ for $k \neq l$. This implies that the auxiliary Gaussian variables X_a, X_b, Y_a, and Y_b are independent.

Note that the behavior of the crosstalk noise differs from that of the ASE. To show this, consider a hypothetical pulse with $g_k = 1$ for $k \neq 1, -1$, and $g_{-1} = g_1 = 1$, so that $\sigma_1 = \sigma_{-1}$. Then, $u = D_{1r} + D_{2r} = 1/2(X_a + N_{-1})(X_b + N_1) + 1/2(X_a + M_{-1})(X_b + M_1)$. Assume also, for simplicity, that $\langle X_a \rangle = \langle X_b \rangle = 0$, i.e., $c_0 = 0$. Hence, $u = D_{1r} + D_{2r}$ is of the form $u = 1/2 u_1 u_2 + 1/2 u_3 u_4$, where the u_i are zero mean Gaussian random variables. Note that the moments $\langle u^n \rangle$ of u depend on the correlation of the u_i. For example $\langle u^2 \rangle = \langle (u_1 u_2)^2 \rangle / 4 + \langle (u_3 u_4)^2 \rangle / 4 + \langle (u_1 u_2 u_3 u_4) \rangle / 2$. In the presence of the white ASE noise alone before the optical filter, the u_i are independent. If the crosstalk noise was also white before the optical filter, then the u_i would still be independent and $\langle u^2 \rangle = (\sigma_1^2 + \sigma^2)^2 / 4$. However, considering the actual statistical properties of the crosstalk noise, the variables u_1 and u_3 are correlated and $\langle u_i u_3 \rangle = \langle X_a^2 \rangle = \sigma^2$. One also has $\langle u_2 u_4 \rangle = \sigma^2$, and hence, $\langle u^2 \rangle = (\sigma_1^2 + \sigma^2)^2 / 4 + \sigma^4 / 2$. Hence, $\langle u^2 \rangle$ turns out to be different in the two cases and this can be verified for $\langle u^n \rangle$ with $n > 2$, as well. This suggests that the behavior of the in-band crosstalk noise is different from that of a white noise and care must be taken when computing the MGF of D in the presence of both the ASE and the crosstalk noises.

C. Estimation of the MGF of the Decision Variable

To complete the estimation of the MGF, the expected value of (24) with respect to X_a, X_b, Y_a, and Y_b must be considered. Applying the independence of X_a, X_b, Y_a, and Y_b, the expected value of (24) becomes

$$M_D(s) = \left\langle M_{D|C}(s) \right\rangle = C(s) M_X(s) M_Y(s) \tag{29}$$

where $M_X(s)$ and $M_Y(s)$ are given by

$$M_X(s) = \left\langle \exp\left(A(s) \left[X_a^2 + X_b^2 \right] + B(s) X_a X_b \right) \right\rangle \tag{30a}$$

$$M_Y(s) = \left\langle \exp\left(A(s) \left[Y_a^2 + Y_b^2 \right] + B(s) Y_a Y_b \right) \right\rangle. \tag{30b}$$

The expectations (30a), (30b) involve the calculation of 2D integrals of a function of the form $e^{p(x,y)}$ where $p(x, y)$ is a second-order polynomial with respect to x and y. These integrals can be computed using (20), and the result for $M_D(s)$ is

$$\begin{aligned} M_D(s) &= M_0(s) \\ &= \frac{C(s)}{\left(1 - 2A(s)\sigma^2\right)^2 - \left(B(s)\sigma^2\right)^2} \\ &\quad \times \exp\left(\frac{c_0^2 \left[2A(s) + B(s) \right]}{1 - \left(2A(s) + B(s) \right) \sigma^2} \right) \end{aligned} \tag{31}$$

in the case where $\theta_{ma} - \theta_{mb} = 0$.

$$\begin{aligned} M_D(s) &= M_\pi(s) \\ &= \frac{C(s)}{\left(1 - 2A(s)\sigma^2\right)^2 - \left(B(s)\sigma^2\right)^2} \\ &\quad \times \exp\left(\frac{c_0^2 \left[2A(s) - B(s) \right]}{1 - \left(2A(s) - B(s) \right) \sigma^2} \right) \end{aligned} \tag{32}$$

in the case where $\theta_{ma} - \theta_{mb} = \pi$. Equations (31) and (32) are the required MGFs of the decision variable of a DPSK receiver, taking into account both the ASE and the in-band crosstalk noises.

Note that since $A(s) = A(-s)$, $B(s) = -B(-s)$, and $C(s) = C(-s)$, it turns out that $M_0(s) = M_\pi(-s)$, and hence, $f_0(x) = f_\pi(-x)$, where $f_0(x)$ and $f_\pi(x)$ are the pdfs of D in the case $\theta_{ma} - \theta_{mb} = 0$ and $\theta_{ma} - \theta_{mb} = \pi$, respectively. The EP is given by

$$p_e(a) = \frac{1}{2} \left(\int_{-\infty}^{a} f_0(x) dx + \int_{a}^{\infty} f_\pi(x) dx \right). \tag{33}$$

The optimum threshold is found by differentiating p_e with respect to a, and setting the derivative equal to zero. The optimum threshold $a = a_{\text{opt}}$ that minimizes $p_e(a)$ is found to obey $f_0(a_{\text{opt}}) - f_\pi(a_{\text{opt}}) = 0$, i.e., $f_0(x)$ and $f_\pi(x)$ intersect at the optimum threshold. Due to the symmetry of $f_0(x)$ and $f_\pi(x)$, illustrated in Fig. 2, it is deduced that the optimum threshold is in fact $a_{\text{opt}} = 0$. The minimum EP p_e is therefore given by

$$p_e = \int_{-\infty}^{0} f_0(x) dx = P_0(0) \tag{34}$$

where $P_0(y) = P(D < y | \theta_a - \theta_b = 0)$ is the cumulative distribution function (cdf) of D when $\theta_a - \theta_b = 0$. To estimate

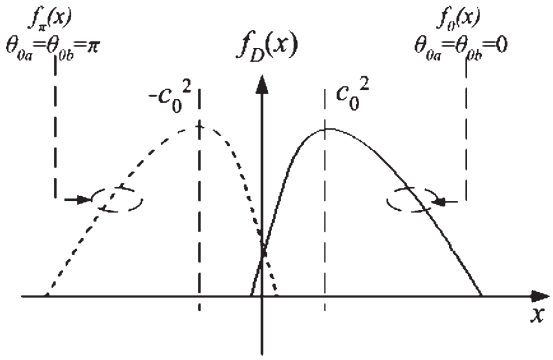

Fig. 2. Symmetry of pdf of the decision variable of the DPSK receiver limited by in-band crosstalk noise.

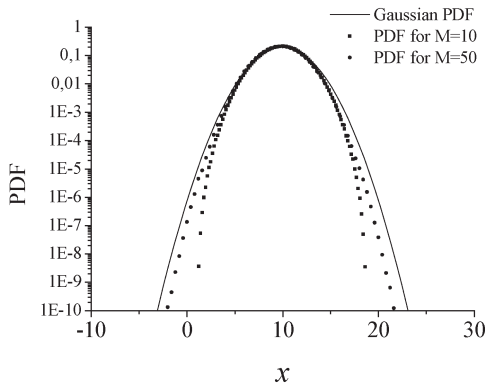

Fig. 3. Convergence of the pdf of D to its asymptotic form as the number of interferers M increases.

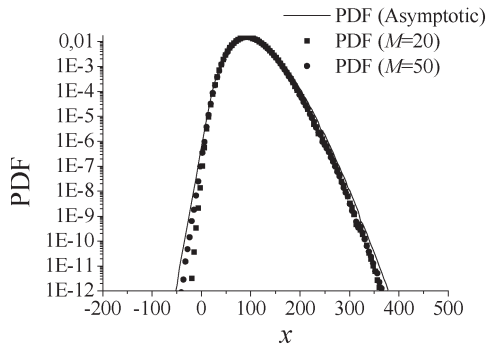

Fig. 4. Convergence of the pdf of X_a to its asymptotic Gaussian form as the number of interferers M increases.

$P_0(a)$, the saddle point approximation along with (31) can be used. As will be shown in the next section, in the absence of ASE noise, the EP can be evaluated in closed form, yielding the error floor set by the in-band crosstalk noise.

Although the present analysis assumes identical pulse shapes $g(t)$ for the signal and interfering components, it is useful to briefly sketch how the theory can be generalized to incorporate nonidentical pulses shapes. If $g_m(t)$ are the pulse shapes of the signal $(m = 0)$ and the crosstalk components $(m > 0)$, one can expand $g_m(t)$ in terms of its Fourier coefficients g_{mk} instead of g_k as in (11). One can then derive an equation similar to (16) where the expressions for x_{ka}, x_{kb}, y_{ka}, and y_{kb} now involve the coefficient g_{mk} instead of g_k. For example, $x_{ka} = \sum_m c_m g_{mk} e_{ma} \cos(\phi_m)$. Equation (23) is valid provided the new values for $\mathbf{z} = \{x_{1a}, \ldots, x_{ka}, x_{kb}, y_{ka}, y_{kb}, \ldots\}$ are taken into account. The variables $\mathbf{z}$ are dependent Gaussian random variables with combined pdf given by $(2\pi)^{-M/2} S^{-1/2} \exp(-1/2 \mathbf{z}^{\mathrm{T}} G \mathbf{z})$, with S and G being the determinant and the inverse of the covariance matrix. To estimate the expectation of (23), one writes $\langle M_{D|C}(s) \rangle$ as $C(s) \langle \exp(\mathbf{z}^{\mathrm{T}} V(s) \mathbf{z}) \rangle = C(s) \int d\mathbf{z} \exp(\mathbf{z}^{\mathrm{T}} K(s) \mathbf{z})$, where $K(s) = V(s) - 1/2G$ is a Hermitian matrix. This integral can be, in principle, estimated by diagonalizing $K(s)$ and one can then evaluate p_e by the saddle point approximation. The detailed analysis and the presentation of the related results is quite lengthy and could be the subject of another publication.

V. Error Floor Due to In-Band Crosstalk Noise

To estimate the error floor due to the in-band crosstalk noise, the ASE noise is neglected (i.e., $\sigma_k = 0$). The decision variable reduces D to

$$D = G_H (X_a X_b + Y_a Y_b) \tag{35}$$

that is, in the absence of optical amplification and as $M \to \infty$, D is the sum of two independent random variables $X_a X_b$ and $Y_a Y_b$, each of which is the product of two independent Gaussian random variables. To verify that D indeed has this asymptotic behavior, the behavior of both D and the auxiliary variables for finite M is considered. The pdf of X_a is illustrated in Fig. 3, for $\phi_0 = 0$ and $M = 10$, 50, along with a Gaussian pdf with mean value m_{xa} and variance equal to σ. The amplitude of the signal c_0 is taken equal to 10, while $\sigma^2 = 4$. The interfering components all have the same amplitude, i.e., for $m > 0$, $c_m = c_1 = (2/M)^{1/2} \sigma$. To estimate the pdf of X_a for finite M, the multicanonical Monte Carlo (MCMC) method was used. As in conventional Monte Carlo sampling, the MCMC method generates samples of the random variable and estimates the pdf from the occurrences of the samples. The sample-generation procedure consists of many iterations. In the first iteration, conventional Monte Carlo sampling is performed to obtain an estimate of the pdf of X_a. The information gained is used in the next iteration to bias the samples and increase the occurrence of the values of X_a at the tails of its pdf. The computed pdf is then used to further bias the samples and so on. This procedure allows the accurate computation of the pdf even at very low values, without an excessive number of samples. The details of this method can be found in [15]–[17]. Fig. 3 clearly illustrates the asymptotic convergence of the pdf of X_a to its asymptotic Gaussian form. Although for $M = 10$ there is some difference between the actual and the asymptotic (Gaussian) pdfs of X_a, this difference is significantly reduced for $M = 50$. A Gaussian assumption was made for the auxiliary variables used in the case of a direct detection ASK receiver in [10] as well. The two auxiliary variables in that case are similar to the ones defined here, except for the e_{ma} and e_{mb}, which are absent in [10]. Nevertheless, the convergence of the auxiliary random variables in Fig. 3 further corroborates the practical importance of the assumption of [10] for finite M.

The convergence of D to its asymptotic form, is illustrated in Fig. 4, where the MCMC method is used to obtain the pdf of

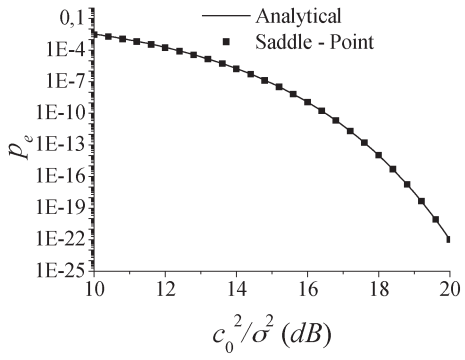

Fig. 5. Comparison of the results obtained by the saddle point method (rectangles) and (33) (solid line).

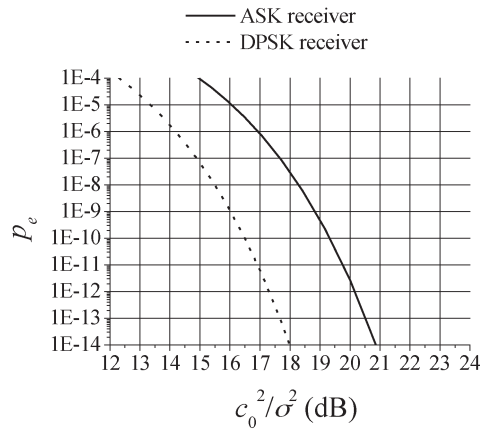

Fig. 6. Error probabilities for an ASK (solid line) and a DPSK (dashed line) receiver for various values of the signal to crosstalk ratio c_0^2/σ^2.

D in the case where $M = 20$ and $M = 50$. The amplitude of the signal and the crosstalk components are again $c_0 = 10$ and $c_m = c_1 = (2/M)^{1/2}\sigma$, respectively, with $\sigma = 2$. Also plotted in Fig. 4 is the asymptotic pdf of D obtained by the MCMC method, assuming that X_a, X_b, Y_a, and Y_b are uncorrelated Gaussian random variables with mean values and standard deviations determined by (14) and (15), respectively. It is observed that as expected, the pdf of D for finite M converges to the pdf of the sum of two independent random variables, each of which is the product of two independent Gaussian random variables.

Note that as M increases, the left tails of the pdf are moving to the left, and hence, for $M \to \infty$, the value of the EP can be higher than for small values of M, especially in the case $M = 1$ that was examined in [11]. This behavior was also observed in the case of ASK modulation [7].

The probability $P(D < 0)$ for such a random variable can be estimated in a closed form as in [18]. Applying the results of [18] in the present case, the minimum EP is given by

$$p_e = \frac{1}{2}\exp\left(-\frac{c_0^2}{2\sigma^2}\right). \tag{36}$$

The MGF of the decision of D in the absence of the ASE noise can be computed by setting $\sigma_k = 0$. In this case, $A(s)$, $B(s)$, and $C(s)$ are given by

$$A(s) = 0 \tag{37a}$$

$$C(s) = 1 \tag{37b}$$

$$B(s) = sG_H \tag{37c}$$

where

$$G_H = \frac{1}{2}\sum_k |g_k|^2 = \frac{1}{2T}\int_{-\infty}^{+\infty} |g_H(t)|^2\, dt. \tag{38}$$

The MGF (31) of the decision variable in the case $\theta_{ma} - \theta_{mb} = 0$, reduces to

$$M_D(s) = M_0(s) = \frac{1}{1-\sigma^4 s^2}\exp\left(\frac{c_0^2\sigma^2 s}{1-\sigma^2 s}\right). \tag{39}$$

Fig. 5 plots the results for the EP calculated by (33), which are compared with the application of the saddle point approximation and (39). It is observed that both methods agree very well, even for very low values of the EP. This result implies that the MGF (31), from which (39) is derived as a special case, is indeed accurately estimated.

It is useful to compare the error floor of the DPSK and the ASK receivers due to the presence of in-band crosstalk. In the case of the ASK receiver, the decision variable D is asymptotically written as the sum of the squares of two auxiliary random variables $c_0 B_0 + R$ and V [10], given by

$$R = c_0 B_0 + \sum_{m\geq 1} B_m c_m \cos\phi_m, \quad V = \sum_{m\geq 1} B_m c_m \sin\phi_m \tag{40}$$

where B_m (equal to 0 or 1) is the bit value of the signal (for $m = 0$) and of the mth crosstalk component (for $m > 0$). It can be shown that the decision variable asymptotically becomes a chi-square random variable [10] with MGF given by

$$M_{\mathrm{ASK}}(s) = \frac{1}{1-\sigma^2 s}\exp\left(\frac{c_0^2 B_0 s}{1-\sigma^2 s}\right) \tag{41}$$

where $\sigma^2 = \langle R^2\rangle + \langle V^2\rangle$ is again given by (27). Note, that in the case of ASK, unlike the DPSK receiver, no analytic result can be obtained for the error floor, since the pdfs of the decision variable for $B_0 = 0$ and $B_0 = 1$ are not symmetric. As a consequence, the optimum threshold position is not known *a priori*. One alternative is to apply the saddle point approximation in order to calculate the optimum threshold and the minimum EP numerically.

In Fig. 6, the value of the error floor due to in-band crosstalk is plotted for the ASK and the DPSK receivers for various values of the signal to crosstalk ratio $SX = c_0^2/\sigma^2$. It is evident that the in-band crosstalk noise affects the ASK receiver more. In fact, for $P_e = 10^{-9}$, the required signal-to-crosstalk ratio for the DPSK receiver $\cong$ 16.1 dB and is about 3 dB lower than that of the ASK receiver. Note that this 3-dB improvement is similar to the improvement encountered in the case when only the ASE noise is present [13].

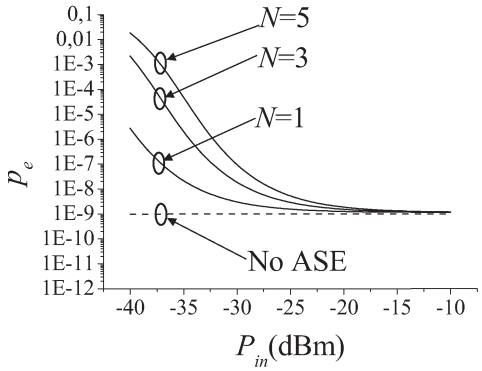

Fig. 7. Influence of the ASE in the EP of a DPSK receiver. N denotes the number of amplifiers that the signal passes.

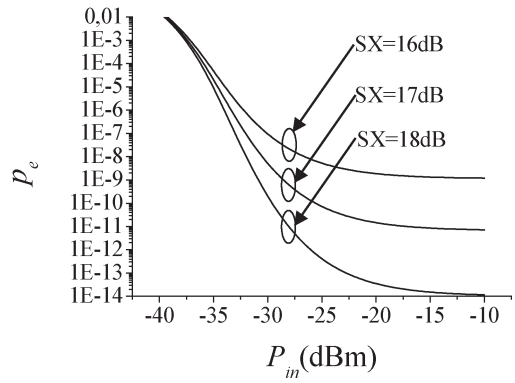

Fig. 8. EP of a preamplified DPSK receiver for three different values of the signal-to-crosstalk ratio SX.

If all interferers have the same amplitude, then $SX = c_0^2/\sigma^2 = 2X/M$, where $X = c_0^2/c_1^2$. In the case of a passive AWG $L \times L$ interconnection, the number of interfering components M, equals $L-1$ [3]. Hence, if DPSK is employed, the receiver at each node can tolerate twice as much in-band crosstalk-noise power, and hence, the maximum number of nodes L that can be interconnected is approximately doubled.

VI. Influence of the ASE Noise

For simplicity, it can be assumed that the pulses $g_H(t)$ are normalized so that $G_H = 1$. If $g_H(t)$ takes negligible values outside $[0, T]$, then G_H can be approximated by

$$G_H \cong \frac{1}{2T}\int_{-\infty}^{+\infty} |g_H(t)|^2\, dt = \frac{1}{2T}\int_{-\infty}^{+\infty} |G(f)|^2\, |H(f)|^2\, df. \tag{42}$$

In (42), $G(f)$ and $H(f)$ are the Fourier transform of $g(t)$ and the transfer function of the optical receiving filter, respectively. The second equality holds as a consequence of Parseval's identity [14], and since $G(f)H(f)$ is the Fourier transform of $g_H(t)$. If $G(f)$ is much narrower than $H(f)$, then $G(f)H(f) \cong G(f)$ (i.e., the optical filter does not significantly alter the pulse spectrum), then

$$\frac{1}{2T}\int_0^T |g(t)|^2\, dt \cong G_H = 1 \tag{43}$$

which means that the normalization of $g(t)$ is approximately the same as that of $g_H(t)$. The energy of the optical field $S_0(t)$ in $[0, T]$ is given by $1/2\int_0^T |S_0(t)|^2 dt$. Taking into account (43), it is easy to deduce that Tc_0^2 is the number of photons of the signal at the output of the optical amplifier. Similarly, Tc_m^2, for $m > 0$, is the number of photons of the mth crosstalk component.

The influence of the ASE noise is illustrated in Fig. 7, where the EP of a DPSK receiver is plotted as a function of the input power $P_{\rm in}$ at the input of the optical amplifier. The signal-to-crosstalk ratio is assumed $SX = 16.1$ dB, which corresponds to an error floor equal to 10^{-9}. The optical amplifier is assumed to have $G = 30$ dB and $n_{\rm sp} = 1$. The optical filter is assumed rectangular with bandwidth W_o equal to 100 GHz, i.e., $H(f) = 1$ for $|f| \le W_{\rm o}/2$. Since Tc_0^2 is the number of photons of the signal inside the bit duration, and if, for simplicity, $g_H(t)$ is assumed rectangular inside $[0, T]$, then $P_{\rm in}T/(hf) = Tc_0^2$ and $c_0^2 = P_{\rm in}/(hf)$. In the figure, N denotes the number of optical amplifiers that the signal and the crosstalk components pass before reaching the receiver's optical filter. The last amplifier is that of the preamplified receiver, and in the case $N = 1$, only this amplifier is assumed. Also plotted in the figure is the error floor of the crosstalk noise obtained using (36). For low input powers, the ASE noise is dominant, especially if $N > 1$. As $P_{\rm in}$ increases, the EP is improved because the ASE noise power is reduced compared to the signal power. However, the EP cannot improve beyond 10^{-9}, which is the error floor set by the in-band crosstalk noise.

In Fig. 8, the EP is plotted for various values of the signal-to-crosstalk ratio SX for $N = 5$. It is deduced that the EP is severely affected by the value of SX, even in the presence of the ASE noise. Indeed, if SX is increased by 1 dB, from 16 to 17 dB, the EP can vary by about two orders of magnitude depending on the input power. It should also be noted that the in-band crosstalk noise does not simply set an error floor but can significantly affect the relation between the EP and the input power, even if the EP is several orders larger than the error floor. This is evident in Fig. 8, since the value of SX influences the rate in which the EP is decreased as $P_{\rm in}$ increases. It is therefore verified that the crosstalk noise can have important implications in the performance of the receiver even in the presence of ASE noise.

VII. Conclusion

In this paper, the influence of the in-band crosstalk in a DPSK was theoretically investigated. An expression for the MGF of the decision variable that takes into account the ASE noise of the optical amplifiers was derived. This expression for the MGF, along with the saddle point approximation, provides a useful model for the evaluation of the EP in DPSK receivers in the presence of in-band crosstalk noise. A closed-form formula for the error floor set by the in-band crosstalk noise was also given.

REFERENCES

[1] R. Ramaswmami and K. Sivarajan, *Optical Networks: A Practical Perspective*, 1st ed. San Mateo, CA: Morgan Kaufmann, 1998.

[2] D. J. Blumenthal, P. Granestrand, and L. Thylen, "BER floors due to heterodyne coherent crosstalk in space photonic switches for WDM networks," *IEEE Photon. Technol. Lett.*, vol. 8, no. 2, pp. 284–286, Feb. 1996.

[3] H. Takahashi, K. Oda, and H. Toba, "Impact of crosstalk in an arrayed-waveguide multiplexer on N × N optical interconnection," *J. Lightw. Technol.*, vol. 14, no. 6, pp. 1098–1105, Jun. 1996.

[4] I. T. Monroy and E. Tangliongga, "Performance evaluation of optical cross-connects by saddlepoint approximation," *J. Lightw. Technol.*, vol. 16, no. 3, pp. 317–323, Mar. 1998.

[5] E. Iannone, R. Sabella, M. Avattaneo, and G. de Paolis, "Modeling of in-band crosstalk in WDM optical networks," *J. Lightw. Technol.*, vol. 17, no. 7, pp. 1138–1141, Jul. 1999.

[6] K. P. Ho, "Analysis of homodyne crosstalk in optical networks using Gram–Charlier series," *J. Lightw. Technol.*, vol. 17, no. 2, pp. 149–154, Feb. 1999.

[7] T. Kamalakis, T. Sphicopoulos, and M. Sagriotis, "Accurate error probability estimation in the presence of in-band crosstalk noise in WDM networks," *J. Lightw. Technol.*, vol. 21, no. 10, pp. 2172–2181, Oct. 2003.

[8] T. Kamalakis and T. Sphicopoulos, "Application of the saddle point method for the evaluation of crosstalk implications in an arrayed waveguide grating interconnection," *J. Lightw. Technol.*, vol. 20, no. 8, pp. 1357–1366, Aug. 2002.

[9] X. Jiang and I. Roudas, "Asymmetric probability density function of a signal with interferometric crosstalk," *IEEE Photon. Technol. Lett.*, vol. 13, no. 2, pp. 160–162, Feb. 2001.

[10] T. Kamalakis and T. Sphicopoulos, "Asymptotic behavior of in-band crosstalk noise in WDM networks," *IEEE Photon. Technol. Lett.*, vol. 15, no. 3, pp. 476–479, Mar. 2003.

[11] X. Liu, Y.-H. Kao, M. Movassaghi, and R. C. Giles, "Tolerance to in-band coherent crosstalk of differential phase-shift-keyed signal with balanced detection and FEC," *IEEE Photon. Technol. Lett.*, vol. 16, no. 4, pp. 1209–1211, Apr. 2004.

[12] X. Liu, "Nonlinear effects in phase shift keyed transmission," presented at the Optical Fiber Communication (OFC), Los Angeles, CA, 2004, Paper ThM4.

[13] G. Einarsson, *Principles of Lightwave Communications*. New York: Wiley, 1996.

[14] P. M. Morse and H. Feshbach, *Methods of Theoretical Physics Part I*. New York: McGraw-Hill, 1953, p. 456.

[15] D. Yevick, "Multicanonical communication system modeling—Application to PMD statistics," *IEEE Photon. Technol. Lett.*, vol. 14, no. 11, pp. 1512–1514, Nov. 2002.

[16] D. P. Landau and K. Binder, *A Guide to Monte Carlo Simulations in Statistical Physics*. Cambridge, U.K.: Cambridge Univ. Press, 2002.

[17] T. Kamalakis, D. Varoutas, and T. Sphicopoulos, "Statistical study of in-band crosstalk noise using the multi-canonical Monte Carlo method," *IEEE Photon. Technol. Lett.*, vol. 16, no. 10, pp. 2242–2244, Oct. 2004.

[18] J. G. Proakis, *Digital Communications*. New York: McGraw-Hill, 1989.

[19] I. S. Gradshteyn and I. M. Ryzhik, *Table of Integrals Series and Products*, 6th ed. San Diego, CA: Academic, 2000.

Thomas Kamalakis was born in Athens, Greece, in 1975. He received the B.Sc. degree in informatics and the M.Sc. degree in telecommunication with distinction, from the University of Athens in 1997 and 1999, respectively. In 2004, he completed his thesis in the design and modeling of arrayed waveguide grating (AWG) devices leading to the Ph.D. degree.

He is currently a Research Associate of the Optical Communications Laboratory of the University of Athens, and an Assistant Lecturer in electronics for the University of Peloponnese, Greece. He serves as a Consultant for the deployment of optical fibers in the Peloponnese district and had participated in the OTEWAVE project of the National Telecommunication Organization of Greece, which dealt with the integration of IP and wavelength-division multiplexing (WDM). His research interests include photonic-crystal devices and nonlinear effects in optical fibers.

Thomas Sphicopoulos (M'87) received the degree in physics from Athens University, Athens, Greece, in 1976, the D.E.A. and Doctorate in Electronics degrees both from the University of Paris VI, France, in 1977 and 1980, respectively, and the Doctorat Es Science degree from the Ecole Polytechnique Federale de Lausanne, Lausanne, Switzerland, in 1986.

From 1976 to 1977, he worked in Thomson CSF Central Research Laboratories on microwave oscillators. From 1977 to 1980, he was an Associate Researcher with the Thomson CSF Aeronautics Infrastructure Division. In 1980, he joined the Electromagnetism Laboratory, Ecole Polytechnique Federal de Lausanne, where he carried out research on applied electromagnetism. Since 1987, he has been with Athens University, engaged in research on broadband communications systems. In 1990, he was elected as an Assistant Professor of Communications in the Department of Informatics and Telecommunications, in 1993, as Associate Professor, and since 1998, as a Professor in the same department. His main scientific interests are microwave and optical communication systems and networks and technoeconomics. He has led about 40 national and European research and development (R&D) projects. He has more than 100 publications in scientific journals and conference proceedings. From 1999, he has been an Advisor for several organizations, including the Greek national regulatory authority (NRA) for telecommunications (EETT), in the fields of market liberalization, spectrum-management techniques, and technology convergence.